Supporting Information

van Dongen et al. 10.1073/pnas.1201072109

SI Materials and Methods

Participant Screening and Inclusion Criteria. Participants were screened in advance for the presence of neurological and psychological disorders, drug use, and MR scanner compatibility through questionnaires. In addition, before inclusion in this study, an inventory was made of each participant's sleeping habits. Participants were included only if they had habitual bedtimes between 10 PM and 1 AM, were used to falling asleep on their back, had no sleep disorders, and reported no recurrent problems sleeping during the month leading up to the experiment. All participants followed normal sleep schedules in the three nights leading up to the experiment but were partially sleep deprived during the last night before the experiment. Participants were instructed to wake up 4 h earlier than normal on their day of participation. Adherence to these instructions was confirmed by using wrist-mounted activity monitors (ActiGraph) and sleep logs. Participants were asked not to consume caffeine or alcohol starting on the night before the experiment. Participants who were included underwent the reactivation protocol for at least 80% in slow-wave sleep (SWS), did not report hearing any sounds during the sleep period, and did not show any microarousals on the EEG during reactivation.

Psychomotor Vigilance Task (PVT). The PVT is a test of sustained attention and has been shown to be sensitive to sleepiness (1, 2). As such, we administered this task before and after the sleep period to check for possible differences in overall vigilance. During the PVT, a target stimulus would appear at random intervals on an otherwise empty screen. At the same time, a counter below the target stimulus would start to scroll. Participants were instructed to respond by pressing a button on the keyboard as fast as possible as soon as the target appeared. After a response, the counter displayed the reaction time for 1 s, providing the subject with feedback on performance. Interstimulus intervals were distributed randomly from 2 to 10 s; the task lasted 10 min (2). The PVT error rate was defined by the number of lapses (RT > 500 ms) plus false alarms (button presses when no target was present).

Object-Location Task. We adapted the object-location task of Rudoy and colleagues (3) for use in an fMRI setting. All learning and testing took place in the MR scanner. Participants first learned the location of pictures of everyday objects. During the initial phase of the learning period, 50 pictures of everyday objects were displayed onto a projection screen (screen size: 47 × 35 cm, resolution: 1024 × 768, viewing distance: 60 cm) for 3,000 ms followed by a 1,000-ms blank interstimulus interval. Sounds were 500 ms in duration and were presented simultaneously with the onset of the corresponding object through MR-compatible earphones. Each object was presented at a screen location randomly determined for each object and each participant. A grid background was provided as reference, but objects could appear anywhere on the screen. After this round of passive viewing, a phase of active learning started. During active learning, an object would appear at the center of the screen while its sound was presented, and the participant attempted to place the object on its original location by using an MR-compatible joystick (Current Designs). Learning trials were self-paced and terminated after the participant confirmed the object placement by button press. The object was then displayed in the correct location for 3,000 ms.

Participants completed several rounds of learning with objects in random order. For every round, objects were excluded from the learning list if they were placed <4 cm from the correct location on the two preceding rounds (average number of rounds to criterion: 11; range: 6–29). When this criterion was reached for all objects, participants took a final test with all objects ("pre-sleep test"). During this test, object placement was not followed by feedback, but instead with an interstimulus period of fixation with a duration jittered between 3,000 and 5,000 ms (the "fixation baseline"). Accuracy on this test provided presleep memory results; an identical test was taken after the sleep period ("post-sleep test") to measure postsleep memory performance.

Polysomnography Acquisition and Analysis. During the sleep period, EEG was recorded at a sampling frequency of 5 kHz by using a 0.1-Hz high-pass filter and a 250-Hz low-pass filter. Electrodes were placed at 31 scalp sites (Fp1, Fp2, F3, F4, C3, C4, P3, P4, O1, O2, F7, F8, T7, T8, P7, P8, Fz, Cz, Pz, POz, Oz, FC1, FC2, CP1, CP2, FC5, FC6, CP5, CP6, TP9, TP10). After recording, EEG data were corrected for gradient and pulse artifacts offline as described by Allen et al. (4, 5) and implemented in Vision Analyzer 2.0 (Brain Products). A 25-volume, baseline corrected sliding average was used for the correction of the gradient artifacts. The average pulse artifact was calculated based on a sliding average, time-locked to the R peak present in the bipolar electrocardiogram. This sliding average was scaled to an optimum least-squares fit for each heart beat by using the scaling option in Vision Analyzer before it was subtracted from the data. Thereafter, EEG data were high-pass filtered at 0.3 Hz, low-pass filtered at 35 Hz, and downsampled to 250 Hz. Afterward, each 30-s epoch was manually scored as wake (W), sleep stage 1 (N1), sleep stage 2 (N2), slow-wave sleep (N3), or rapid eye movement sleep (R) by experts according to standard criteria (6).

fMRI Data Acquisition. Participants were scanned during the presleep learning and test session, throughout the sleep period, and during the postsleep test session. We used a reduced-noise echo-planar imaging (EPI) sequence that makes use of sinusoidal gradients, which avoid the acoustic resonances of the scanner (7). T2*-weighted images were acquired covering the whole brain [28 axial slices, ascending slice acquisition, repetition time (TR) = 2,511 ms, echo time (TE) = 38 ms, 90° flip angle, matrix = 64 × 64, bandwidth = 1,502 Hz per pixel, slice thickness = 3.5 mm, slice gap = 15%, field of view (FOV) = 224 mm]. For structural MRI, T1-weighted images were acquired with a magnetization prepared, rapid-acquisition gradient echo sequence (176 sagittal slices, TR = 2,250 ms, TE = 2.95 ms, 15° flip angle, matrix = 256 × 256, slice thickness = 1.0 mm, FOV = 256 mm). Participants' heads were fixed in a firm but comfortable manner to prevent movement.

Reactivation Protocol. During the sleep period, the polysomnographic recordings were corrected for MR artifacts online by using BrainProducts RecView 1.4 (BrainProducts). The corrected EEG was continuously monitored for signs of slow-wave sleep. When two experimenters rated the current EEG as representative of stable N3 sleep, presentation of the sounds was manually initiated. Sound stimuli consisted of 25 sound stimuli previously presented during the learning phase ("cue sounds") and 5 control stimuli with the same duration (guitar strums, "control sounds"). Presentation of both cue and control sounds during the reactivation period occurred in 5-trial blocks. Within each block, the interstimulus interval was jittered between 4,000 and 8,000 ms, for an average block duration of 32.5 s. Blocks consisted of

a random arrangement of five stimuli from the same condition (i.e., cue or control sounds). Each cue stimulus was presented twice, for a total of 50 cue events. The control sounds were presented five times, for a total of 25 control events. The stimulation volume was set for each participant individually by using the results from the volume test conducted before the learning period. Sounds were presented through plug-in earphones that also functioned as earplugs to minimize the impact of the continuous scanner noise.

Cue sounds were selected such that the memory performance for object locations at baseline test was matched for cued and uncued (sounds not used during the sleep session) conditions.

fMRI Data Preprocessing. Image preprocessing and statistical analysis was done by using SPM8. The first five volumes of each functional EPI run were discarded to allow for T1 equilibration. An outlier algorithm was first used to check for and replace corrupted slices from each image volume by using between-volume interpolation. Thereafter, motion correction was performed by using iterative rigid body realignment to minimize the residual sum of squares between the first and all further functional scans. Next, the participant's mean functional image was coregistered with the corresponding structural MR image by using mutual information optimization. All functional images were then corrected for geometric distortions along the phase encoding direction by using constrained nonlinear coregistration (8). Data were subsequently spatially normalized and transformed into Montreal Neurological Institute space (resampled at voxel size $2 \times 2 \times 2$ mm^3), as defined by the SPM8 EPI.nii template. Finally, the functional scans were spatially filtered by convolving them with an isotropic 3D Gaussian kernel (8 mm full width at half maximum). For the analysis of the sleep period, the normalized functional images were segmented into gray matter, white matter, and cerebral spinal fluid (CSF) areas by using the unified segmentation algorithm implemented in SPM8 (9). These segmented images were used as masks to calculate mean intensity levels for white matter, CSF, and a residual compartment (the section outside the brain and skull) for each functional image. The segmentation procedure was performed to create three compartment regressors to account for any residual movement or signal intensity-related effects in the BOLD signal (10).

fMRI Data Analysis of the Testing Sessions. The fMRI data were analyzed statistically by using the general linear model (GLM) and statistical parametric mapping. For the test session scans, the explanatory variable included all 50 retrieval trials. Each trial was modeled as a single event of 0 duration and temporally convolved with the canonical hemodynamic response function (HRF) along with its temporal derivatives provided by SPM8. Each event was time-locked to the presentation of the object. The design matrix additionally included the six head motion regressors (translations, rotations). A high-pass filter was implemented by using a cutoff period of 128 s to remove low-frequency effects from the time series. For statistical analysis, relevant parameter images were generated for each subject for the contrast between retrieval trials and the (implicit) fixation baseline. Participant-specific contrast parameter images were subsequently subjected to a second-level analysis treating subjects as a random variable (11).

fMRI Data Analysis of the Sleep Period. The fMRI data were analyzed statistically by using the GLM and statistical parametric mapping. For the sleep period scans, two explanatory variables were included: cue sounds (presentation of sounds previously associated with object-location associations learned presleep) and control sounds (presentation of sounds not associated with objects from the object-location task). All trials were modeled as events with 5-s durations and temporally convolved with the canonical HRF along with its temporal and dispersion derivatives provided by SPM8. Each event was time-locked to the presentation of the auditory stimulus. The design matrix further included the six head motion regressors (translations, rotations), their derivatives, and three compartment parameters. A high-pass filter was implemented by using a cutoff period of 128 s to remove low-frequency effects from the time series. To restrict the analysis to physiologically plausible regions of the brain a gray matter mask, based on the gray matter segment of the SPM8 EPI.nii template, was used during the first-level analysis. For statistical analysis, relevant contrast parameter images were generated for each subject and subsequently subjected to a second-level analysis treating subjects as a random variable (11).

Functional Connectivity Analysis. Based on the results obtained in the cue > control sounds contrast, we focused our analysis on the functional connectivity of the right parahippocampal cortex during slow-wave sleep. For this purpose we used a psychophysiological interaction (PPI) analysis (12, 13). PPI analyses explore the influence of a psychological factor on the coactivation between a seed region of interest and the rest of the brain. We investigated whether presentation of cues or control sounds (the psychological factor) during slow-wave sleep modified parahippocampal connectivity patterns (the physiological factor). We defined our functional region of interest (ROI) in the right parahippocampal cortex by using the cue > control contrast. All voxels in the right parahippocampal cortex that showed significantly increased activity (at $P < 0.01$, uncorrected) to presentation of cues compared with control sounds were extracted by using SPM8. Next, the BOLD signal within this parahippocampal ROI was extracted during the sleep period by using its first eigenvector. We then searched for an interaction between the physiological variable (parahippocampal time course) and the psychological context (cue or control sound presentation). For each participant, a second GLM was constructed containing regressors for the general deconvolved signal of the seed region (physiological factor), the onsets of the cue and control events (psychological factor), and the interaction between physiological and psychological factors. The participant-specific contrast parameter images generated by this third regressor were used as input for second-level analysis treating subjects as a random variable.

Correlational Analysis. To probe the relationship between cue-induced BOLD responses and the behavioral effect of the reactivation protocol, we included a covariate in the second-level random effects analyses of the activity and connectivity differences between cue and control sound presentation. This covariate contained for each participant the average difference in performance between the pre- and postsleep test for associations cued during the sleep period. Thus, this parameter quantified the behavioral effect of the reactivation protocol on each participant's accuracy in the cued condition.

fMRI Analysis of the Activity Changes from the Pre- to Postsleep Test. The fMRI data were analyzed statistically by using the general linear model (GLM) and statistical parametric mapping. For the test session scans, two explanatory variables (cued and uncued) were included, each consisting of 25 retrieval trials. Each trial was modeled as a single event of 0 duration and temporally convolved with the canonical hemodynamic response function (HRF) along with its temporal derivatives provided by SPM8. Each event was time-locked to the presentation of the object. The design matrix additionally included the six head motion regressors (translations, rotations). A high-pass filter was implemented by using a cutoff period of 128 s to remove low-frequency effects from the time series. For statistical analysis, relevant parameter images were generated for each subject for each session for the contrast between cued and uncued trials. Participant-specific contrast pa-

rameter images for each session were subsequently subjected to a second-level paired comparison to investigate possible changes in activity from the pre- to postsleep test. Additionally, a covariate was added to the second level containing for each participant the average difference in performance between the pre- and postsleep test for associations cued during the sleep period. No significant differences in activity were found between the cued and uncued stimuli at the pre- and postsleep test, nor did we observe a significant change of such activity across the sleep period. Differences in activity were, moreover, not significantly correlated with the behavioral covariate.

fMRI Analysis of the Connectivity Changes from the Pre- to Postsleep Test. Here, we investigated whether retrieval of cued or uncued associations (the psychological factor) during the object location task modified parahippocampal connectivity patterns (the physiological factor). We defined our functional region of interest (ROI) in the parahippocampal cortex by using the cue > control contrast from the sleep data. All voxels in the parahippocampal cortex within a 10-mm sphere from the peak parahippocampal activation in the SWS cues > control contrast were extracted by using SPM8. This procedure created a right parahippocampal ROI centered around [32 −42 −6] that was subsequently mirrored in the x dimension to create a ROI for the left parahippocampus centered at [−32 −42 −6]. These ROIs were then combined into one bilateral parahippocampal ROI. Next, the BOLD signal within this ROI was extracted during the presleep and postsleep retrieval task by using its first eigenvector. We then searched for an interaction between the physiological variable (parahippocampal time course) and the psychological context (cued or uncued association retrieval). For each participant, a second GLM was constructed containing regressors for the general deconvolved signal of the seed region (physiological factor), the onsets of the cued and uncued retrieval trials (psychological factor), and the interaction between physiological and psychological factors. The participant-specific contrast parameter images generated by this third regressor were used as input for second-level analysis treating subjects as a random variable. Additionally, a covariate was added to the second level containing for each participant the average difference in performance between the presleep and postsleep test for associations cued during the sleep period.

This analysis showed that at the postsleep test parahippocampal–medial prefrontal connectivity (related to retrieval of cued associations) was positively correlated with the effect of the reactivation protocol. No such effect was visible at the presleep test, even at lower statistical thresholds ($P < 0.01$ uncorrected). We then used the participant-specific contrast parameter images for each session to conduct a second-level paired comparison to investigate possible changes in parahippocampal connectivity from the pre- to postsleep test. We restricted our analysis to the medial prefrontal region based on the postsleep test results. This analysis demonstrated that parahippocampal connectivity with the medial prefrontal region increased from the pre- to postsleep test. Furthermore, an interaction was observed between the effect of the reactivation protocol, parahippocampal–medial prefrontal connectivity, and testing session. Better retention of cued associations was positively correlated with pre- to postsleep changes in parahippocampal–medial prefrontal connectivity during retrieval of reactivated associations. These results are visualized in Fig. 4*C* and documented in Tables S6 and S7.

Statistical Thresholding. Unless otherwise reported, contrast images were initially thresholded at $P < 0.001$ uncorrected, with subsequent family-wise error (FWE, $P < 0.05$) correction for multiple comparisons at the cluster or small-volume level.

1. Dorrian JR, Rogers NL, Dinges DF (2005) Psychomotor vigilance performance: A neurocognitive assay sensitive to sleep loss. *Sleep Deprivation: Clinical Issues, Pharmacology and Sleep Loss Effects*, ed Kushida C (Marcel Dekker, New York), pp 39–70.
2. Drummond SP, et al. (2005) The neural basis of the psychomotor vigilance task. *Sleep* 28:1059–1068.
3. Rudoy JD, Voss JL, Westerberg CE, Paller KA (2009) Strengthening individual memories by reactivating them during sleep. *Science* 326:1079.
4. Allen PJP, Polizzi G, Krakow K, Fish DR, Lemieux L (1998) Identification of EEG events in the MR scanner: The problem of pulse artifact and a method for its subtraction. *Neuroimage* 8:229–239.
5. Allen PJ, Josephs O, Turner R (2000) A method for removing imaging artifact from continuous EEG recorded during functional MRI. *Neuroimage* 12:230–239.
6. Iber C, Ancoli-Israel S, Chesson A, Quan SF (2007) *The AASM Manual for the Scoring of Sleep and Associated Events: Rules, Terminology and Technical Specifications* (Am Acad Sleep Med, Westchester, IL).
7. Schmitter S, et al. (2008) Silent echo-planar imaging for auditory FMRI. *MAGMA* 21: 317–325.
8. Visser E, Qin S, Zwiers M (2010) EPI distortion correction by constrained nonlinear coregistration improves group fMRI. *Proc Intl Soc Mag Reson Med* 18:3459.
9. Ashburner J, Friston KJ (2005) Unified segmentation. *Neuroimage* 26:839–851.
10. Verhagen LG, Grol MJ, Dijkerman HC, Toni I (2006) Studying visually guided reach to grasp movements in an MR-environment. *Neuroimage* 31:S45.
11. Penny W, Friston K (2003) Mixtures of general linear models for functional neuroimaging. *IEEE Trans Med Imaging* 22:504–514.
12. Friston K (1994) Functional and effective connectivity in neuroimaging: A synthesis. *Hum Brain Mapp* 1:56–78.
13. Friston KJ, et al. (1997) Psychophysiological and modulatory interactions in neuroimaging. *Neuroimage* 6:218–229.

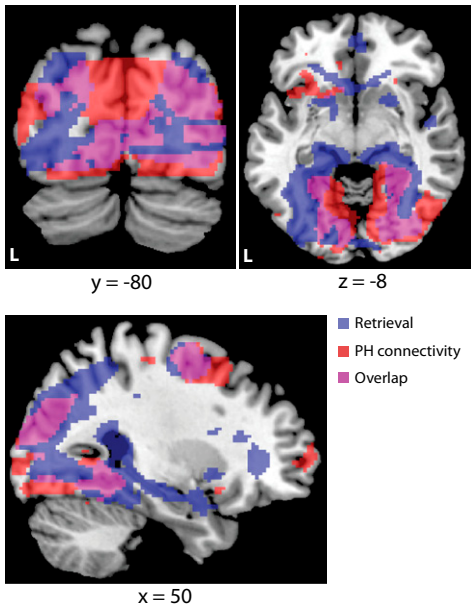

Fig. S1. Overlap between retrieval activity during the presleep test (blue) and parahippocampal connectivity that increased during presentation of cue sounds (red). Overlays are plotted at a threshold of $T > 2.0$ on the single subject template brain of Mricron (http://www.mccauslandcenter.sc.edu/mricro/mricron/index.html). PH, parahippocampus; L, left.

Table S1. Polysomnographic parameters of the sleep period

Sleep parameter	Time (min ± SEM)	Percentage (% ± SEM)
W	13.9 (3.2)	11.0 (2.3)
N1	15.5 (3.1)	11.9 (1.9)
N2	42.5 (5.4)	33.7 (3.7)
N3	50.4 (5.2)	43.3 (4.6)
Total sleep time	108.4 (4.9)	88.9 (2.3)
Sleep period length	122.3 (4.9)	100

W, Wake; N1/N2/N3, stage 1/2/3 sleep.

Table S2. Object location task fMRI: Retrieval vs. baseline

					MNI coordinates		
	Size in voxels	Peak T	Significance	Area	*X*	*Y*	*Z*
Cluster 1	6272	8.76	$P < 0.001$	L parahippocampal gyrus	**−30**	**−50**	**−10**
				R parahippocampal gyrus	30	−46	−10
				L lingual gyrus	−8	−80	-4
				R cuneus	12	−90	16
				R superior parietal lobule	26	−66	44
				L mid occipital gyrus	−22	−84	14
				L cuneus	−4	−90	2
				R lingual gyrus	24	−76	−2
				R precuneus	24	−58	28
				L precuneus	−20	−64	30
Cluster 2	293	7.05	$P = 0.003$	L anterior cingulate cortex	**−18**	**36**	**2**
				L inferior frontal gyrus	−24	30	−4
Cluster 3	749	6.90	$P < 0.001$	L posterior cingulate cortex	**−8**	**−44**	**10**
				R posterior cingulate cortex	8	−42	10
				L hippocampus	−12	36	8
				R hippocampus	26	−20	−14
				R parahippocampal gyrus	20	−24	−16
Cluster 4	264	5.73	$P = 0.006$	L precentral gyrus	**−36**	**−22**	**58**
Cluster 5	329	5.49	$P = 0.002$	L superior frontal gyrus	**−24**	**−4**	**60**
				L medial frontal gyrus	−12	−2	58
Cluster 6	187	5.31	$P = 0.028$	L parahippocampus	**−20**	**−22**	**−14**
				L hippocampus	−32	−14	−18

Brain activity during the presleep object-location task that increased with retrieval of object-locations associations compared to baseline. For each cluster, all local maxima in distinct anatomical regions are listed. Results are obtained after initial thresholding at $P < 0.001$ uncorrected at the voxel level, followed by FWE correction for multiple comparisons at the cluster level at $P < 0.05$. The cluster maximum for each cluster is denoted in bold. L, left; R, right.

Table S3. Reactivation during SWS: Functional connectivity of the right parahippocampal cortex during presentation of cue vs. control sounds

					MNI coordinates		
	Size in voxels	Peak T	Significance	Area	*X*	*Y*	*Z*
Cluster 1	7132	8.94	$P = 0.001$	R parahippocampal gyrus	**32**	**−42**	**−8**
				L precuneus	−4	−56	10
				R precuneus	4	−56	8
				L lingual gyrus	−2	−74	0
				R lingual gyrus	26	−50	−10
				R calcarine gyrus	4	−98	12
				L cuneus	−18	−66	20
				R posterior cingulate cortex	20	−56	4
Cluster 2	481	4.90	$P = 0.002$	L precuneus	**−10**	**−50**	**54**
				R precuneus	4	−42	48
				R paracentral lobule	2	−48	56
				R cingulate gyrus	10	−46	28
Cluster 3	283	4.98	$P = 0.02$	L middle temporal gyrus	**−38**	**−74**	**18**
				L angular gyrus	−44	−72	30

Parahippocampal connectivity in SWS that was stronger during presentation of cue compared with control sounds. No significant increases in connectivity were observed when comparing control with cue sounds. Results are obtained after initial thresholding at $P < 0.001$ uncorrected at the voxel level, followed by FWE correction for multiple comparisons at the cluster level at $P < 0.05$. The cluster maximum for each cluster is denoted in bold. For each cluster, all local maxima in distinct anatomical regions are listed. L, left; R, right.

Table S4. Reactivation during SWS fMRI: Cue-related activity correlated with a positive reactivation effect across participants

					MNI coordinates		
	Size in voxels	Peak T	Significance	Area	*X*	*Y*	*Z*
Cluster 1	452	6.55	$P = 0.001$*	R thalamus	**4**	**10**	**−4**
				L thalamus	−10	−28	−2
Cluster 2	409	4.92	$P = 0.001$*	L cerebellum	**−2**	**−68**	**−28**
				R cerebellum	6	−58	−20
Cluster 3	298	7.75	$P = 0.007$*	L cerebellum	**−28**	**−48**	**−44**
Cluster 4	74	5.64	$P = 0.003$**	L hippocampus	**−36**	**−12**	**−18**
				L insula	−36	−4	−14
Cluster 5	41	4.63	$P = 0.009$***	R parahippocampal gyrus	**24**	**−24**	**−18**

Cue-related brain activity (as specified in the contrast between cue and control sounds) in SWS that across participants was correlated with a positive effect of the reactivation protocol. No brain activity was significantly correlated with negative reactivation outcome. Results are obtained after initial thresholding at $P < 0.001$ uncorrected at the voxel level. For each cluster, all local maxima in distinct anatomical regions are listed. The cluster maximum for each cluster is denoted in bold. L, left; R, right.

*P value significant at $P < 0.05$ after FWE correction at the cluster level.

**P value significant at $P < 0.05$ after FWE correction at the small volume level, using a 10-mm sphere centered at the nearest cluster of hippocampal activation [−32 −14 −18] observed in the contrast between retrieval and baseline activity.

***P value significant at $P < 0.05$ after FWE correction at the small volume level, using a 10-mm sphere centered at the nearest cluster of parahippocampal activation [20 −24 −16] observed in the contrast between retrieval and baseline activity.

Table S5. Reactivation during SWS: Functional connectivity of the right parahippocampal cortex related to a positive effect of reactivation across participants

					MNI coordinates		
	Size in voxels	Peak T	Significance	Area	*X*	*Y*	*Z*
Cluster 1	485	5.33	$P = 0.002$	R precuneus	**20**	**−66**	**34**
				L precuneus	−8	−74	44

Cue-related parahippocampal connectivity in SWS that across participants was correlated with a positive effect of the reactivation protocol. No significant correlations between connectivity and negative reactivation outcome were observed. Results are obtained after initial thresholding at $P < 0.001$ uncorrected at the voxel level, followed by FWE correction for multiple comparisons at the cluster level at $P < 0.05$. The cluster maximum for each cluster is denoted in bold. For each cluster, all local maxima in distinct anatomical regions are listed. L, left; R, right.

Table S6. Functional connectivity during the postsleep test: Connectivity of the parahippocampal cortex related to a positive effect of reactivation across participants

					MNI coordinates		
	Size in voxels	Peak T	Significance	Area	*X*	*Y*	*Z*
Cluster 1	443	5.28	$P < 0.001$	R superior medial gyrus	**8**	**62**	**16**
				R mid orbital gyrus	10	52	−2
				R anterior cingulate cortex	12	48	−10

Cued associations-related parahippocampal connectivity during the postsleep test that correlated with a positive effect of the reactivation protocol. No significant correlations between connectivity and negative reactivation outcome were observed. Results are obtained after initial thresholding at $P < 0.001$ uncorrected at the voxel level, followed by FWE correction for multiple comparisons at the cluster level at $P < 0.05$. The cluster maximum is denoted in bold. For each cluster, all local maxima in distinct anatomical regions are listed. R, right.

Table S7. Pre- to postsleep test changes in parahippocampal connectivity during retrieval

	Size in voxels	Peak T	Significance	Area	MNI coordinates		
					X	*Y*	*Z*
Main effect							
Cluster 1	11	4.83	$P = 0.032$	L superior medial gyrus	**−12**	**54**	**4**
Cluster 2	28	4.52	$P = 0.016$	R anterior cingulate cortex	**14**	**42**	**4**
Cluster 3	8	4.36	$P = 0.038$	R superior medial gyrus	**10**	**60**	**14**
Interaction effect							
Cluster 1	7	4.22	$P = 0.040$	L superior medial gyrus	**−12**	**54**	**4**

Main effect: cued associations-related parahippocampal connectivity that increased from pre- to postsleep test. No significant decreases in connectivity were observed. Interaction effect: cued associations-related parahippocampal connectivity of which the increase from pre- to postsleep test correlated with the positive effect of reactivation. No significant correlations between connectivity and negative reactivation outcome were observed. Results are obtained within the mPFC ROI from Table S6 with initial thresholding at $P < 0.001$ uncorrected at the voxel level, followed by FWE correction for multiple comparisons at the cluster level at $P < 0.05$. For each cluster, all local maxima in distinct anatomical regions are listed. L, left; R, right.